Identification of a natural soluble neuropilin-1 that binds vascular endothelial growth factor: *In vivo* expression and antitumor activity

Michael L. Gagnon*†, Diane R. Bielenberg*†, Ze'ev Gechtman*, Hua-Quan Miao*, Seiji Takashima‡, Shay Soker§, and Michael Klagsbrun*¶‖

Departments of *Surgical Research, ¶Pathology, and §Urology, Children's Hospital and Harvard Medical School, 300 Longwood Avenue, Boston, MA 02115; and ‡First Department of Medicine, Osaka University Hospital, Yamadaoka 2-2, Suita, Osaka 565, Japan

Edited by Robert Langer, Massachusetts Institute of Technology, Cambridge, MA, and approved December 17, 1999 (received for review August 10, 1999)

Neuropilin-1 (NRP1) is a 130-kDa transmembrane receptor for semaphorins, mediators of neuronal guidance, and for vascular endothelial growth factor 165 ($VEGF_{165}$), an angiogenesis factor. A 2.2-kb truncated NRP1 cDNA was cloned that encodes a 644-aa soluble NRP1 (sNRP1) isoform containing just the a/CUB and b/coagulation factor homology extracellular domains of NRP1. sNRP1 is secreted by cells as a 90-kDa protein that binds $VEGF_{165}$, but not $VEGF_{121}$. It inhibits ^{125}I-$VEGF_{165}$ binding to endothelial and tumor cells and $VEGF_{165}$-induced tyrosine phosphorylation of KDR in endothelial cells. The 3′ end of sNRP1 cDNA contains a unique, 28-bp intron-derived sequence that is absent in full-length NRP1 cDNA. Using a probe corresponding to this unique sequence, sNRP1 mRNA could be detected by *in situ* hybridization differentially from full-length NRP1 mRNA, for example, in cells of liver, kidney, skin, and breast. Analysis of blood vessels *in situ* showed that NRP1, but not sNRP1, was expressed. sNRP1 was functional *in vivo*. Unlike control tumors, tumors of rat prostate carcinoma cells expressing recombinant sNRP1 were characterized by extensive hemorrhage, damaged vessels, and apoptotic tumor cells. These results demonstrate the existence of a naturally occurring, soluble NRP1 that is expressed differently from intact NRP1 and that appears to be a $VEGF_{165}$ antagonist.

tumor angiogenesis | prostate carcinoma cells | apoptosis | receptor

Neuropilin-1 (NRP1) is a transmembrane glycoprotein, first described in the developing nervous system, that is expressed on axons of dorsal root ganglia, sensory, and motor neurons (1). NRP1 is a receptor for several members of the semaphorin/collapsin family, negative mediators of neuronal guidance (2, 3). NRP1 was shown by us also to be an isoform-specific receptor for vascular endothelial growth factor (VEGF) that binds $VEGF_{165}$ but not $VEGF_{121}$ to the surface of endothelial cells (EC) and tumor cells (4). $VEGF_{165}$ is an EC mitogen *in vitro* and angiogenesis factor *in vivo* whose activities are mediated by the VEGF tyrosine kinase receptors Flt-1 (VEGFR1) and Flk-1/KDR (VEGFR2) (reviewed in refs. 5–8). Expression of NRP1 in EC enhances the binding of $VEGF_{165}$ to KDR and $VEGF_{165}$-induced EC chemotaxis (4). Thus, it appears that in EC, NRP1 acts as a coreceptor that enhances KDR activity. The involvement of NRP1 in angiogenesis is supported by the observation that overexpression of NRP1 in transgenic mice results in excess capillary and blood vessel formation (9). The consequences of $VEGF_{165}$ binding to tumor cell NRP1 have not yet been determined. A role for semaphorin interactions with NRP1 in angiogenesis has been suggested by the ability of semaphorin III/collapsin-1, an inhibitor of axonal motility, to inhibit the migration of EC in a NRP1-dependent manner (10). Inhibition of EC motility is associated with the depolymerization of F-actin and retraction of lamellipodia in a manner similar to growth cone collapse.

In our initial Northern blot analysis of NRP1 gene expression, we noticed that besides the predominant 7-kb mRNA species, smaller, 2.2- to 2.5-kb mRNA species were also expressed by PC3 prostate carcinoma cells, heart, and placenta (4). In this report, we describe the cloning of a 2.2-kb NRP1 cDNA that encodes a truncated, 644-aa soluble neuropilin-1 (sNRP1) isoform. Purified, 90-kDa sNRP1 binds $VEGF_{165}$ but not $VEGF_{121}$ and appears to be a $VEGF_{165}$ antagonist. A unique, 28-bp sNRP1 intron-derived sequence at the 3′ end that allows *in situ* hybridization analysis of sNRP1 distinct from full-length NRP1 shows that the expression patterns of these two NRP1 isoform mRNAs differ. Overexpression of sNRP1 in tumor cells *in vivo* is associated with increased tumor cell apoptosis. These results demonstrate that a natural NRP1-soluble receptor exists that may function as a $VEGF_{165}$ antagonist.

Materials and Methods

Cell Culture and Animals. AT2.1 and AT3.1 rat prostate carcinoma cells (11) were provided by Bruce Zetter (Children's Hospital, Boston) and grown in RPMI 1640 medium containing 10% FCS and L-glutamine/penicillin G/streptomycin sulfate (GPS) (Irvine Scientific). Human PC3 prostate carcinoma cells were provided by Michael Freeman (Children's Hospital) and grown in RPMI 1640/10% FCS/GPS. Chinese hamster ovary cells (CHO-K1) were obtained from American Type Culture Collection and cultured in F12 medium with 10% FCS/GPS. Porcine aortic EC expressing NRP1 (PAE-NRP1) and both NRP1 and KDR (PAE/NRP1/KDR) have been described previously (4). Pathogen-free male Copenhagen rats were purchased from Charles River Laboratories and used at 10 weeks of age.

Northern Blot Analysis. Poly(A)$^+$ RNA preparation, RNA gel electrophoresis, blotting, and hybridization were performed as described (12). Probes were made from PCR products corresponding to the entire human a/CUB (754 bp), b/factor V/VIII (950 bp), and c/MAM (488 bp) NRP1 domains (13) and amplified by using the following primers, respectively: 5′a, TTCGCAACGATAAATGTGGCG; 3′a, GAAATCTTCT-

This paper was submitted directly (Track II) to the PNAS office.

Abbreviations: NRP1, neuropilin-1; sNRP1, soluble neuropilin-1; VEGF, vascular endothelial growth factor; EC, endothelial cells; CM, conditioned medium; ISH, *in situ* hybridization; PCNA, proliferating cell nuclear antigen; TUNEL, terminal deoxynucleotidyltransferase-mediated dUTP nick end labeling.

Data deposition: The sequence reported in this paper has been deposited in the GenBank database [accession no. AF145712 (soluble neuropilin-1 cDNA)].

†M.L.G. and D.R.B. contributed equally to this work.

‖To whom reprint requests should be addressed at: Department of Surgical Research, Children's Hospital, 300 Longwood Avenue, Boston, MA 02115. E-mail: klagsbrun@a1.tch.harvard.edu.

The publication costs of this article were defrayed in part by page charge payment. This article must therefore be hereby marked "*advertisement*" in accordance with 18 U.S.C. §1734 solely to indicate this fact.

Article published online before print: *Proc. Natl. Acad. Sci. USA*, 10.1073/pnas.040337597. Article and publication date are at www.pnas.org/cgi/doi/10.1073/pnas.040337597

GAGACACTGC; 5′b, GAAGATTTCAAATGTATGGAAG; 3′b, GGCTTCCACTTCACAGCCCAG; 5′c, GGTTTTAACTGTGAATTTGG; 3′c, ACAATCTTCTTGTGAAATGTG.

An oligonucleotide (TTCTGTCACATTTCGTATTTTATTTGATACTTTTTCG) that was complementary to the sNRP1 intron-derived sequence was also used as a probe by using the 3DNA Probe ^{32}P kit (Genisphere, Oakland, NJ).

Human sNRP1 cDNA Cloning. A natural, soluble NRP1 cDNA was cloned by 3′ RACE (rapid amplification of cDNA ends) as described previously (12). First-strand oligo(dT)-primed cDNA was synthesized from 2 μg of PC3 mRNA, and PCR was performed by using primers 5′b and *Bam*HI-dT (CCCTTCGGATCCTAACCTTTTTTTTTTTTTTTT); a secondary PCR was performed by using the first PCR as template and primers 5′b2 (GAAGTATACGGTTGCAAGATA) and *Bam*HI (CCCTTCGGATCCTAACC). A 700-bp PCR product was cloned by using the TOPO TA Cloning kit (Invitrogen). The 3′ cDNA clone sequence was identified as a truncated NRP1 (sNRP1) cDNA.

Expression Vectors. The complete sNRP1 cDNA subsequently was cloned by PCR from the PC3 cDNA reaction and ligated into the pcDNA3.1 mammalian expression vector (Invitrogen). This sNRP1-pcDNA3.1 plasmid consisted of the entire 1,932-bp ORF and included the first 16 of 28 bp of intron-derived sequence at the 3′ end. For purification purposes, an H/m-sNRP1-pcDNA3.1 plasmid was constructed that contained His and c-Myc domain tags (HHHHHHQQKLISQQNL) between P^{36} and G^{37}.

Immunoblot Analysis. Cell lysates and serum-free conditioned medium (CM) were adjusted to 0.5 M NaCl/1 mM $MnCl_2$/1 mM $CaCl_2$ and incubated with 75 μl of 50% wt/vol Con A Sepharose beads (Amersham Pharmacia) overnight at 4°C with rotation. Con A beads were washed three times in 0.5 M NaCl/20 mM Tris, pH 7.5, and once in 50 mM NaCl/20 mM Tris, pH 7.5. Con A-binding proteins were separated by 7.5% SDS/PAGE and transferred to 0.45-μm Protran nitrocellulose membranes (Schleicher & Schuell). Membranes were incubated with 1:500 dilutions of either a rabbit polyclonal antibody (41-1), immunoreactive against amino acids 22-41 near the N terminus of human NRP1, or a goat polyclonal antibody (C-19) immunoreactive against the C-terminal 19 aa of NRP1 (Santa Cruz Biotechnology). Horseradish peroxidase-conjugated secondary anti-rabbit IgG (Roche Diagnostics, Indianapolis, IN) and monoclonal anti-goat IgG (Sigma) were used at a 1:5,000 dilution, and blots were developed by using an enhanced chemiluminescence kit (NEN).

Synthesis and Purification of Recombinant sNRP1 Protein. The H/m-sNRP1-pcDNA3.1 plasmid was transfected into Chinese hamster ovary (CHO-K1) cells by using Lipofectamine Reagent (Life Technologies, Gaithersburg, MD). A G418-resistant, sNRP1-expressing clone, as determined by Western blot with the 41–1 antibody, was expanded and used to condition 3 liters of serum-free medium. CM was concentrated by using an Amicon filter (Millipore), adjusted to 20 mM Tris, pH 7.5/0.5 M NaCl/1 mM $MnCl_2$/1 mM $CaCl_2$ (Con A-binding buffer), and incubated with 5 ml of 50% vol/vol Con A beads overnight at 4°C. The beads were washed with Con A-binding buffer. Con A-binding proteins were eluted with 20 mM Tris, pH 7.5/50 mM NaCl/0.2 M methyl α-D-mannopyranoside at 25°C for 1 hr and applied onto a 1-ml HiTrap chelating column loaded with cobalt and attached to a Pharmacia FPLC system. The column was washed with 20 mM Hepes, pH 7.2/0.5 M NaCl. Bound proteins were eluted by a linear gradient of 5–150 mM imidazole at a 0.5 ml/min flow rate. Fractions were analyzed for the presence of sNRP1 by Western blot analysis and Coomassie blue staining of SDS/PAGE. Pooled sNRP1 fractions were concentrated and adjusted to 20 mM Hepes, pH 7.2/50 mM NaCl.

Binding of ^{125}I-VEGF$_{165}$ to sNRP1 and to Cells. *Binding in solution.* $VEGF_{165}$ and VEGF121 were iodinated as described (14). Five nanograms of ^{125}I-$VEGF_{165}$ or ^{125}I-$VEGF_{121}$ was incubated with 500 ng of purified sNRP1 in 50 mM Hepes, pH 7.2/0.1 M NaCl for 2 hr at 25°C. Complexes were cross-linked in 0.2 mM disuccinimidyl suberate for 30 min, and the reaction was stopped by the addition of 10 mM Tris, pH 7.4/250 mM glycine/2 mM EDTA. Complexes were separated by 6% SDS/PAGE, and dried gels were autoradiographed. For competition experiments, sNRP1 (500 ng) was incubated with 10 ng of ^{125}I-$VEGF_{165}$ in a binding buffer that contained 20 mM Hepes (pH 7.4), 0.1% Tween-20, 0.1% BSA, and 1 μg/ml heparin for 1.5 hr at 24°C in the presence of unlabeled $VEGF_{165}$ or $VEGF_{121}$ (0–4 μg of VEGF, VEGF/^{125}I-$VEGF_{165}$ molar ratio of 0–400). sNRP1/^{125}I-$VEGF_{165}$ complexes were incubated overnight at 4°C with anti-Myc antibodies (5 μg, clone 9E10; Santa Cruz Biotechnology) followed by protein G-Sepharose incubation for 1 hr. Immune complexes were washed three times with the binding buffer, and the associated radioactivity was measured in a γ-counter. Scatchard analysis (4) of these data was used to measure the K_d of sNRP1/$VEGF_{165}$ interactions.

Binding to cells. Binding of ^{125}I-$VEGF_{165}$ (10 ng/ml) to PAE-NRP1 and AT2.1 cells in the presence of 1 μg/ml heparin was performed as described (14, 15). For competition experiments, increasing amounts of sNRP1 (0–5 μg of sNRP1, sNRP1/^{125}I-$VEGF_{165}$ molar ratio of 0–500) were added.

Tyrosine Phosphorylation of KDR. PAS/NRP1/KDR cells were grown in 10-cm plates to 80% confluence and serum-starved overnight in F12 medium supplemented with 0.1% BSA. Cells were treated with 5 ng/ml $VEGF_{165}$ with and without 1 μg/ml sNRP1 for 10 min, washed with ice-cold PBS, and lysed in 1.2 ml of buffer, which contained 20 mM sodium phosphate (pH 7.2), 1% Triton X-100, 50 mM NaCl, 250 mM sucrose, 2 mM EDTA, 1 mM sodium orthovanadate, 10 mM NaF, 5 mM sodium pyrophosphate, and a mixture of protease inhibitors. Cell lysates were precleared by incubation with 40 μl of protein G-Sepharose (50% vol/vol slurry) for 1 hr at 4°C and incubated overnight with 1 μg of polyclonal anti-KDR antibodies (Santa Cruz Biotechnology). The immune complexes were incubated with 40 μl of protein G-Sepharose (50% vol/vol slurry) for 1.5 hr at 4°C, washed four times with lysis buffer, and boiled in 2× Laemmli's sample buffer. Proteins were resolved on 7% SDS/PAGE and analyzed by Western blot by using monoclonal antiphosphotyrosine antibodies (16).

***In Situ* Hybridization Analysis (ISH).** ISH was performed as described (17, 18) with biotinylated oligonucleotide probes (Research Genetics, Huntsville, AL). The biotinylated probes used were an antisense sNRP1-specific oligonucleotide complementary to the 28-nt, intron-encoded 3′ mRNA (TTCTGTCACATTTCGTATTTTATTTGATAC) and a control sense oligonucleotide. After hybridization, slides were stained with Fast Red alkaline phosphatase substrate (Biomeda, Foster City, CA). An antisense NRP1-specific riboprobe was made from a 750-bp 3′ UTR cDNA fragment in Bluescript II KS(+) (Stratagene) by using a digoxigenin RNA-labeling kit (Boehringer Mannheim) and used in ISH as described (19). Slides were stained with BM Purple alkaline phosphatase substrate (Boehringer Mannheim). Probes were hybridized to slides of PC3 cells and NormalGrid:Multi-tissue Control Slides (Biomeda).

Transfection of sNRP1 into Tumor Cells and Tumor Growth *In Vivo*. The sNRP1-pcDNA3.1 or pcDNA3.1 (neo) plasmids were trans-

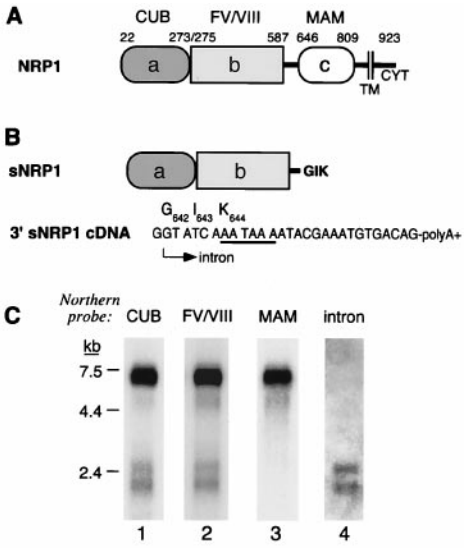

Fig. 1. sNRP1 structure and mRNA. (*A*) Schematic representation adapted from ref. 13 of NRP1. The a/CUB, b/factor V/VIII coagulation factor, and c/MAM homology domains as well as the transmembrane (TM) and cytoplasmic (CYT) domains are indicated. The number represents positions in the ORF corresponding to the boundaries of the various domains. (*B*) Schematic representation of sNRP1. The sNRP1 protein is identical to NRP1 up to Ser^{641}, which is in the linker region between the b/coagulation and c/MAM homology domains and, in addition, contains three novel amino acids, G^{642} I^{643} K^{644}. There is a unique, 28-bp, intron-derived sequence at the 3′ end of the cDNA. The 5′ end (arrow) of this sequence has a GT splice donor site, and its 3′ end is followed by a poly(A)$^+$ tail. The cleavage/polyadenylation site (AATAAA), which contains a TAA stop codon, is underlined. The three new amino acids are shown above the codons. (*C*) Northern blot analysis of PC3 cell mRNA with probes corresponding to the a/CUB domain (lane 1), the b/coagulation factor domain (lane 2), the c/MAM domain (lane 3), and an oligonucleotide probe complementary to the sNRP1 28-bp, intron-derived sequence (lane 4). Each lane was loaded with 2 μg of PC3 mRNA.

fected into AT2.1 or AT3.1 prostate carcinoma cells, and G418-resistant, sNRP1-expressing clones were isolated. Tumor cells [10^6 cells/200 μl of Hanks' balanced salt solution (HBSS)] were injected into Copenhagen rats s.c. in the dorsal lateral flank proximal to the midline or orthotopically (10^6 cells/40 μl of HBSS) into the prostate. Rats were monitored daily and sacrificed 3 weeks after tumor cell injection.

Immunohistochemistry. Formalin-fixed, paraffin-embedded tissues were used for routine histology and immunohistochemistry to identify dividing proliferating cell nuclear antigen (PCNA)-positive cells and terminal deoxynucleotidyltransferase-mediated dUTP end labeling (TUNEL)-positive cells as described (20). The stained tumor slides were scanned by using a Polaroid Sprint Scan35 (Meyer Instruments) to obtain photographs of entire tumor sections.

Results

Identification and Cloning of a 2.2-kb NRP1 Isoform Expressed by PC3 Cells. Human NRP1 is expressed as a 7-kb mRNA transcript in adult cell lines and tissues (4). However, a shorter NRP1 mRNA doublet of 2.2–2.5 kb also was expressed in some cells and tissues, for example, human prostate carcinoma PC3 cells, heart, and placenta. NRP1 has an extracellular domain (13) consisting of complement (a/CUB), coagulation factor V/VIII (b), and MAM (c) homology subdomains (Fig. 1*A*). Northern blots using cDNA probes corresponding to the a/CUB (Fig. 1*C*, lane 1) and b/coagulation factor (Fig. 1*C*, lane 2) homology domains detected both 7-kb and 2.2- to 2.5-kb NRP1 mRNAs, whereas a probe corresponding to the c/MAM homology domain (Fig. 1*C*, lane 3) detected only 7-kb mRNA. These results suggested that the 2.2- to 2.5-kb mRNAs represent isoforms truncated in the extracellular domain. A 2,190-bp NRP1 cDNA was cloned from PC3 cells whose sequence predicted that it would encode a 644-aa truncated NRP1 isoform (Fig. 1*B*). The truncation occurs after NRP1 Ser^{641}, which is located in a linker region between the b/coagulation factor and c/MAM domains, and there are three additional novel amino acids, Gly^{642}-Ile^{643}-Lys^{644}, at the C terminus. The truncated NRP1 cDNA has a presumptive intron sequence at its 3′ end consisting of a unique, 28-bp sequence that contains a GT splice donor consensus sequence at its 5′ end, a TAA stop codon, and a cleavage/polyadenylation site that determines the 3′ end of the mRNA (Fig. 1*B*). Northern blot analysis using a probe complementary to this 28-bp sequence detected 2.2- to 2.5-kb but not 7-kb NRP1 mRNAs (Fig. 1*C*, lane 4).

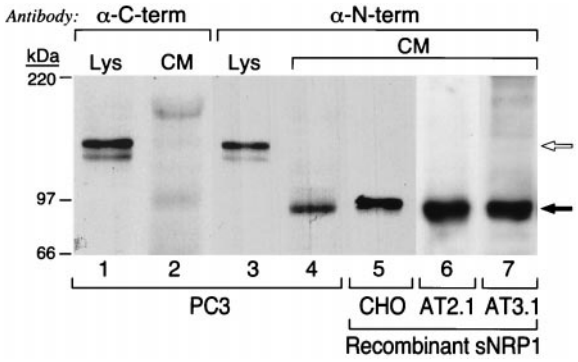

Fig. 2. Western blot analysis of sNRP1 protein expression. PC3 cell lysates (Lys) and CM were partially purified by Con A chromatography, resolved by SDS/PAGE, and probed with anti-NRP1 antibodies directed against the C-terminal (α-C-term) and N-terminal (α-N-term) regions of NRP1. Lanes: 1 and 3, PC3 cell lysates; 2 and 4, PC3 cell CM; 5, CHO cell CM from cells expressing recombinant His/Myc-tagged sNRP1; 6, AT2.1 cell CM from cells expressing recombinant sNRP1; 7, AT3.1 cell CM from cells expressing recombinant sNRP1. The open arrow indicates 130-kDa, full-length NRP1, and the solid arrow indicates 90-kDa sNRP1. The recombinant protein made by CHO cells is slightly larger because it is His- and Myc-tagged.

Synthesis of sNRP1 Protein in PC3 Cells. PC3 cell lysates and CM were analyzed by Western blot (Fig. 2). An antibody specific for the C terminus of the NRP1 cytoplasmic domain (α-C-term) detected a 130-kDa doublet in the lysate (Fig. 2, lane 1) that corresponds to full-length NRP1 but detected no bands in CM (Fig. 2, lane 2). On the other hand, an antibody specific for the N terminus of human NRP1 (α-N-term) detected not only 130-kDa NRP1 in the lysate (Fig. 2, lane 3) but also a single, 90-kDa protein in CM (Fig. 2, lane 4). The 90-kDa protein comigrated with recombinant protein found in the CM of CHO (Fig. 2, lane 5), AT2.1 (Fig. 2, lane 6), and AT3.1 (Fig. 2, lane 7) cells transfected with 2.2-kb sNRP1 cDNA.

sNRP1 Binds ^{125}I-VEGF$_{165}$, Inhibits Its Binding to Cells, and Inhibits VEGF$_{165}$ Activity. His- and Myc-tagged recombinant sNRP1 was purified and appeared as a single band of 90 kDa as detected by SDS/PAGE and Coomassie blue staining (Fig. 3*A*). N-terminal amino acid sequencing of this band yielded the sequence FRND-KCGDTI, corresponding exactly to the first 10 aa after the NRP1 signal peptide (4). Recombinant sNRP1 cross-linked to ^{125}I-VEGF$_{165}$ in solution formed a 120- to 140-kDa doublet complex consistent with the cross-linking of 90-kDa sNRP1 and 35- to 40-kDa VEGF$_{165}$ (Fig. 3*B*, lane 1). sNRP1, however, did not

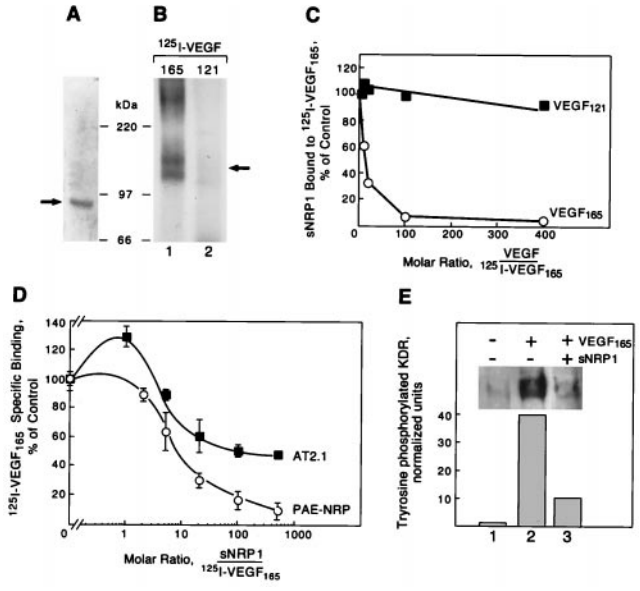

Fig. 3. Recombinant sNRP1 inhibits $VEGF_{165}$ binding and activity. (*A*) Recombinant His/Myc-tagged sNRP1 was purified and analyzed by SDS/PAGE and Coomassie blue staining. A single band of approximately 90 kDa is indicated by a solid arrow. (*B*) sNRP1 (50 ng) was incubated with 5 ng of ^{125}I-$VEGF_{165}$ (lane 1) or ^{125}I-$VEGF_{121}$ (lane 2) in solution, followed by cross-linking with disuccinimidyl suberate, SDS/PAGE, and autoradiography. A 120- to 140-kDa complex is formed with ^{125}I-$VEGF_{165}$ (solid arrow) but not with $VEGF_{121}$. (*C*) His/Myc-tagged sNRP1 (500 ng) was incubated in solution with 10 ng of ^{125}I-$VEGF_{165}$ in the presence of increasing amounts of unlabeled $VEGF_{165}$ (○) or $VEGF_{121}$ (■). sNRP1/^{125}I-$VEGF_{165}$ complexes were immunoprecipitated with anti-Myc antibodies. The relative amounts of sNRP1 bound to ^{125}I-$VEGF_{165}$ were measured in a γ-counter. The counts were normalized and presented as percentage of control. (*D*) ^{125}I-$VEGF_{165}$ (10 ng/ml) was incubated with PAE-NRP1 cells (○) or AT2.1 cells (■) in the absence or the presence of increasing amounts of purified recombinant sNRP1. Cells were lysed and bound ^{125}I-$VEGF_{165}$ was measured in a γ-counter. Each value represents the average of three separate measurements. (*E*) PAE/NRP1/KDR cells were starved overnight and either not treated or treated with 5 ng/ml $VEGF_{165}$ or 5 ng/ml $VEGF_{165}$ plus 1 μg/ml sNRP1 for 10 min. Cells were lysed and KDR was immunoprecipitated with anti-KDR antibodies. The immunoprecipitated proteins were resolved by SDS/PAGE and analyzed by Western blot with antiphosphotyrosine antibodies. Equal amounts of total protein were present in all samples.

form any complex with ^{125}I-$VEGF_{121}$ (Fig. 3*B*, lane 2), consistent with the VEGF isoform specificity of NRP1 (4).

Increasing concentrations of unlabeled $VEGF_{165}$, but not $VEGF_{121}$, inhibited ^{125}I-$VEGF_{165}$ binding to sNRP1 in solution (Fig. 3*C*). Inhibition of 97% was achieved at a molar ratio of unlabeled to labeled $VEGF_{165}$ of 100. Scatchard analysis indicated that sNRP1 binds to $VEGF_{165}$ with a K_d of approximately $5–10 \times 10^{-9}$ M. Full-length NRP1 binds $VEGF_{165}$ with a K_d of approximately 3×10^{-10} M (14). Increasing amounts of recombinant sNRP1 inhibited ^{125}I-$VEGF_{165}$ binding to cells *in vitro* (Fig. 3*D*). ^{125}I-$VEGF_{165}$ binding to PAE-NRP1 and to AT2.1 cells was inhibited by more than 90% and 50%, respectively, at an sNRP1/^{125}I-$VEGF_{165}$ molar ratio of 500.

$VEGF_{165}$-induced tyrosine phosphorylation of KDR in PAE/NRP1/KDR cells was analyzed by immunoprecipitation with anti-KDR antibodies followed by Western blot with antiphosphotyrosine antibodies (Fig. 3*E*). sNRP1 inhibited $VEGF_{165}$-induced tyrosine phosphorylation of KDR by approximately 70%.

Detection of sNRP1 mRNA by ISH Analysis. The sNRP1 28-bp 3′ end sequence is not contained in full-length NRP1 mRNA and is unique as determined by a search of the National Center for Biotechnology Information database. An oligonucleotide complementary to the 28-bp sequence that specifically recognized the 2.2- to 2.5-kb sNRP1 mRNAs as shown by Northern analysis (Fig. 1*C*, lane 4) was used for ISH (Fig. 4). Cultured PC3 cells express sNRP1 mRNA uniformly in the cytoplasm (Fig. 4*A*). There was no signal using a sense oligonucleotide probe as a control (Fig. 4*B*). A full-length NRP1 riboprobe complementary to a 750-nt 3′ UTR sequence that is absent in sNRP1 detected NRP1 in these cells (data not shown). These ISH results confirm Northern blot analysis showing that PC3 cells express NRP1 and sNRP1 mRNA species (Fig. 1*C*).

The distribution of sNRP1 mRNA expression was analyzed in human tissues. In liver, the sNRP1 signal was associated with hepatocytes but not veins or arteries (Fig. 4*C*). In kidney, the signal was associated with distal and proximal tubules but not the glomeruli (Fig. 4*D*). On the other hand, there was no detectable sNRP1 signal in skin (Fig. 4*E*) or breast (Fig. 4*F*). ISH also was carried out for full-length NRP1 mRNA. Unlike sNRP1, NRP1 was expressed in suprabasal keratinocytes and blood vessels of the skin (Fig. 4*G*) and in ductal epithelia and blood vessels of the breast (Fig. 4*H*). NRP1 also was expressed in liver veins and glomerular capillaries (data not shown). There was no staining in tissues with sNRP1 and NRP1 sense probes (data not shown). Taken together, these results demonstrate that sNRP1 and NRP1 have different expression patterns in a number of tissues. They also suggest that NRP1 but not sNRP1 is associated with blood vessels.

Overexpression of sNRP1 cDNA in Tumor Cells. To determine whether sNRP1 is functional *in vivo*, its effects on tumor cell phenotype *in vivo* were analyzed. Dunning rat prostate carcinoma cell lines (11) transfected with sNRP1-pcDNA3.1 secreted sNRP1 as analyzed by Western blot (Fig. 2, lanes 6 and 7). Cells transfected with pcDNA3.1 alone (AT2.1-neo, AT3.1-neo) did not express sNRP1 (data not shown). Tumor cells expressing sNRP1 grew *in vitro* at the same rate as control cells, and there was no visible effect on phenotype. AT2.1 cells expressing sNRP1 (AT2.1-sNRP1) and control AT2.1-neo cells were injected s.c. into rats, and tumors were excised after 3 weeks. AT2.1-sNRP1 tumors were characterized by having a small, outer rim of viable, dividing tumor cells but a large, hemorraghic center filled with fluid and blood (Fig. 5*A*), with very little proliferation occurring as measured by PCNA analysis (Fig. 5*C*) and with mostly apoptotic cells as measured by TUNEL assay (Fig. 5*E*). On the other hand, AT2.1-neo tumors were solid and vascular (Fig. 5*B*), contained a high proportion of proliferating cells (Fig. 5*D*), and showed very little apoptosis (Fig. 5*F*).

AT3.1-neo and AT3.1-sNRP1 cells were injected orthotopically into the prostates of rats, and tumors were excised after 3 weeks. The AT3.1-sNRP1 tumors were mostly TUNEL-positive, with only a thin, outer rim consisting of viable tumor cells (Fig. 5*G*) whereas the AT3.1-neo tumors were mostly TUNEL-negative (Fig. 5*H*).

The distribution of blood vessels was analyzed in these tumors. von Willebrand factor-positive EC were found in the healthy tumor rims but were greatly diminished in the apoptotic centers of the tumors expressing sNRP1 (data not shown). Furthermore, the blood vessels in the TUNEL-positive regions were damaged and disrupted, thereby contributing to hemorrhage (data not shown). Together, these results suggest that sNRP1 expression has an adverse effect on blood vessel number and integrity.

Discussion

Based on the observation that PC3 cells express not only a 7-kb mRNA corresponding to NRP1, but smaller, 2.2- to 2.5-kb mRNA species as well (4), we have identified, cloned, and purified a naturally occurring, soluble NRP1 isoform, sNRP1. Structurally, sNRP1 is a 90-kDa protein that contains the

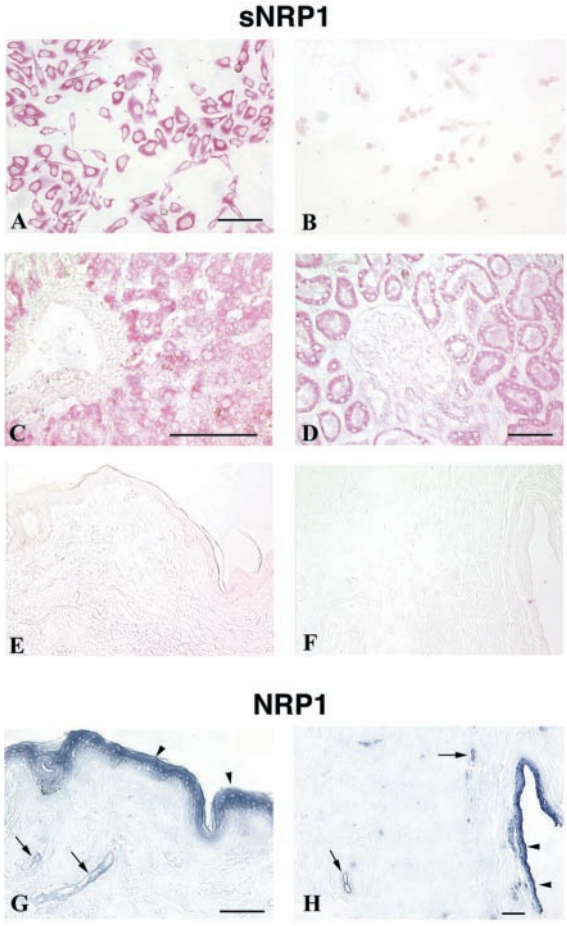

Fig. 4. ISH of sNRP1 and NRP1 mRNA in human cells and tissues. sNRP1 mRNA (red) was detected by ISH by using a sNRP1 oligonucleotide probe complementary to the unique, 28-bp, intron-derived sequence at the 3′ end of the sNRP1 cDNA absent in NRP1. Full-length NRP1 (purple) was detected by ISH by using a 750-nt riboprobe complementary to its 3′ UTR, which is absent in sNRP1. (*A*) sNRP1 in cultured PC3 cells. (*B*) Sense sNRP1 control in cultured PC3 cells. (*C*) sNRP1 in human liver hepatocytes but not in the central vein. (*D*) sNRP1 in human kidney tubules but not glomeruli. (*E*) sNRP1 staining of skin showing no expression. (*F*) sNRP1 staining of breast showing no expression. (*G*) NRP1 in skin suprabasal epidermis (arrowheads) and blood vessels (arrows). (*H*) NRP1 in breast epithelial duct (arrowheads) and blood vessels (arrows). (Bars = 100 μm.)

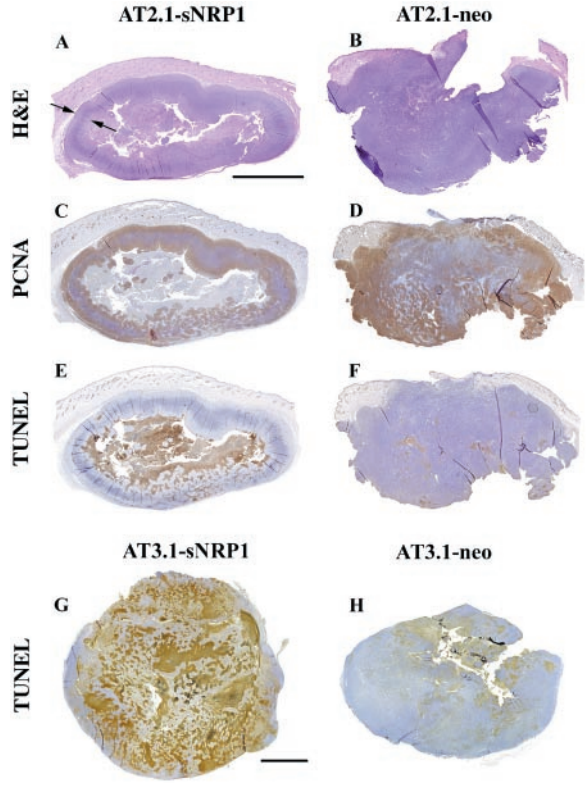

Fig. 5. Tumorigenicity of rat AT2.1 and AT3.1 prostate carcinoma cells transfected with sNRP1. AT2.1 cells expressing sNRP1 (*A*, *C*, and *E*) or control cells with neo vector alone (*B*, *D*, and *F*) were injected s.c. in rats. AT3.1 cells expressing sNRP1 (*G*) or control cells with neo vector alone (*H*) were injected orthotopically into rat prostates. (*A*) Hematoxylin/eosin (H&E) staining. Tumors of cells expressing sNRP1 have a rim (shown between arrows) of normal-looking tumor and a center filled with blood and nonviable cells. (*B*) H&E staining. Control tumors are solid throughout. (*C*) PCNA (brown). Proliferating cells are found only at the outer edge of AT2.1-sNRP1 tumors. (*D*) PCNA. AT2.1-neo tumors contain proliferating cells throughout. (*E–H*) TUNEL assay (brown). The centers of tumors expressing sNRP1 are full of apoptotic cells (*E* and *G*) whereas control tumors have very few areas of apoptosis (*F* and *H*). (Bars = 5 mm.) Similar results were obtained in three independent AT2.1-sNRP1 and AT3.1-sNRP1 clones, each injected into animals in duplicate.

N-terminal a/CUB and b/coagulation factor homology domains but lacks the c/MAM homology, transmembrane, and cytoplasmic domains of full-length, 130-kDa NRP1. NRP1 and sNRP1 are most likely synthesized selectively by the alternative use of cleavage/polyadenylation (C/P) sites within alternatively spliced or unprocessed NRP1 RNA transcripts. Expression of the 2.2-kb sNRP1 mRNA is a result of having a specific C/P site within an intron located upstream of the c/MAM domain of the NRP1 gene. As a consequence, 2.2-kb sNRP1 mRNA contains a unique, 28-bp, intron-derived sequence at the 3′ end. This sequence also contains a stop codon (TAA) resulting in a 644-aa protein that includes three unique amino acids at the C terminus.

Purified sNRP1 binds $VEGF_{165}$ but not $VEGF_{121}$, consistent with the isoform specificity of NRP1 (4). The $VEGF_{165}$-binding site thus is located within the sNRP1 a/CUB and/or b/coagulation factor domains. Consistent with this, deletion analysis of the transmembrane receptor previously has localized the $VEGF_{165}$-binding site to the b/coagulation domain (21). In addition to binding $VEGF_{165}$, sNRP1 potentially could bind various members of the semaphorin family, for example, semaphorin III/collapsin-1, because its binding site within NRP1 has been localized to the a/CUB and b/coagulation domains (21) and it competes with $VEGF_{165}$ for binding (10).

The sNRP1 28-bp, intron-derived 3′ sequence is unique. Its absence in full-length NRP1 mRNA allows detection of sNRP1 distinct from NRP1 in cells and tissues by ISH. We used an ISH technique that utilizes short, biotinylated oligonucleotides (17, 18) and found that sNRP1 mRNA is synthesized in a number of tissues and absent from others. The most significant finding is that NRP1 and sNRP1 gene expression does not overlap. As examples, sNRP1 but not NRP1 mRNA is expressed in liver hepatocytes and kidney distal and proximal tubules. On the other hand, NRP1 but not sNRP1 is expressed in liver veins and glomerular capillaries. NRP1, but not sNRP1, is expressed in skin and breast epithelia and blood vessels. NRP1 was also detected in blood vessels of the heart, brain, skeletal muscle, and placenta. An emerging pattern is that NRP1 is expressed by blood vessels, consistent with its role as an endothelial cell-associated receptor for $VEGF_{165}$, whereas sNRP1 is not. The role of sNRP1 expressed by hepatocytes and kidney tubules is unknown. One possibility is that it acts as a competitive inhibitor of $VEGF_{165}$, preventing its stimulation of EC.

The existence of soluble and intact forms of NRP1 has ramifications for receptor expression analysis. Probes corresponding to 5′ regions and antibodies directed against N termini would not differentiate between sNRP1 and NRP1. This is significant because sNRP1 is an antagonist of $VEGF_{165}$ binding to NRP1 and, thus, the two isoforms could have opposing activities. Earlier studies analyzing the expression of NRP1 during development have used probes that would hybridize to both forms of NRP1 (1, 2). Designing probes for ISH analysis that are specific for the soluble and transmembrane forms of a receptor thus is critical not only for NRP1 but for other receptors that have anchored and soluble forms, such as Flt-1 (22), ErbB1 (23), ErbB3 (24), and FGFR (25).

VEGF-mediated angiogenesis is considered to be a major contributor to tumor growth (26, 27). A number of VEGF antagonists have been developed for the purpose of inhibiting VEGF-induced tumor angiogenesis and tumor growth. These antagonists include VEGF antibodies, dominant-negative receptors, and soluble VEGF receptors (22, 28–32). Native soluble Flt-1 (sFLT-1), a splice variant consisting of six of seven extracellular, Ig-like domains, inhibits VEGF mitogenic activity *in vitro* and tumor formation *in vivo* by sequestering VEGF, thus preventing the ligand from binding to its cell surface receptor (31). sFLT-1 is also capable of acting as a dominant-negative receptor that heterodimerizes with KDR (32). sNRP1 may act in a similar manner. sNRP1 inhibits ^{125}I-$VEGF_{165}$ binding to EC and tyrosine phosphorylation of KDR in EC. To determine whether sNRP1 was functional as an inhibitor *in vivo*, sNRP1 cDNA was overexpressed in Dunning rat prostate carcinoma AT2.1 and AT3.1 cells, which synthesize NRP1 but not sNRP1. The transfectants were injected s.c. or orthotopically into the prostate, and similar results were obtained. The mock transfectants formed tumors that were solid and full of rapidly dividing cells with little evidence of apoptosis. However, tumors arising from sNRP1 transfectants were characterized by the presence of extensive hemorrhage, damaged blood vessels, and massive apoptosis in the tumor centers. Viable cells and intact blood vessels were found only in the outer tumor rim. A possible explanation for this tumor phenotype is that sNRP1 inhibits $VEGF_{165}$-dependent tumor angiogenesis. The effects of sNRP1 on tumor phenotype are similar to those that result from $VEGF_{165}$ withdrawal (33). In these studies, it was demonstrated by using a tetracycline-regulated VEGF expression system that $VEGF_{165}$ withdrawal led to EC death and that the vascular collapse led to hemorrhage and extensive tumor necrosis. There may be other possible mechanisms as well, for example, sNRP1 inhibits ^{125}I-$VEGF_{165}$ binding to rat prostate carcinoma cells, thereby inhibiting direct $VEGF_{165}$ interactions with the tumor cells. The consequences of direct $VEGF_{165}$ interactions with tumor cells is unknown but preliminary results indicate that $VEGF_{165}$ stimulates their motility (H.-Q.M. and M.K., unpublished observations). sNRP1 also might induce apoptosis by sequestering $VEGF_{165}$. It has been demonstrated that $VEGF_{165}$ is a survival factor for EC, and $VEGF_{165}$ withdrawal leads to extensive tumor apoptosis (33).

In summary, we have described a soluble form of NRP1 that is expressed in tissues differentially from NRP1, acts as a $VEGF_{165}$ antagonist, and has antitumor activity. Naturally expressed, soluble VEGF receptors such as sNRP1 and sFLT-1 might constitute a family of proteins that regulate VEGF/VEGF receptor interactions.

We thank Eric Santiestevan and Ricardo Sanchez for excellent technical assistance and Dr. Michael Freeman for the critical reading of the manuscript. These studies were supported by National Cancer Institute Grants CA37392 and CA45548 (M.K.).

1. Takagi, S., Tsuji, T., Amagai, T., Takamatsu, T. & Fujisawa, H. (1987) *Dev. Biol.* **122,** 90–100.
2. He, Z. & Tessier-Lavigne, M. (1997) *Cell* **90,** 739–751.
3. Kolodkin, A. L., Levengood, D. V., Rowe, E. G., Tai, Y. T., Giger, R. J. & Ginty, D. D. (1997) *Cell* **90,** 753–762.
4. Soker, S., Takashima, S., Miao, H. Q., Neufeld, G. & Klagsbrun, M. (1998) *Cell* **92,** 735–745.
5. Klagsbrun, M. & D'Amore, P. A. (1996) *Cytokine Growth Factor Rev.* **7,** 259–270.
6. Ferrara, N. & Davis-Smith, T. (1997) *Endocrine Rev.* **18,** 4–25.
7. Neufeld, G., Cohen, T., Gengrinovitch, S. & Poltorak, Z. (1999) *FASEB J.* **13,** 9–22.
8. Klagsbrun, M. & Moses, M. (1999) *Chem. Biol.* ***6,*** R217–R224.
9. Kitsukawa, T., Shimono, A., Kawakami, A., Kondoh, H. & Fujisawa, H. (1995) *Development* **121,** 4309–4318.
10. Miao, H. Q., Soker, S., Feiner, L., Alonso, J. L., Raper, J. A. & Klagsbrun, M. (1999) *J. Cell Biol.* **146,** 233–241.
11. Isaacs, J. T., Isaacs, W. B., Feitz, W. F. J. & Scheres, J. (1986) *Prostate* **9,** 261–281.
12. Gagnon, M. L., Moy, G. K. & Klagsbrun, M. (1999) *J. Cell. Biochem.* **72,** 492–506.
13. Kawakami, A., Kitsukawa, T., Takagi, S. & Fujisawa, H. (1996) *J. Neurobiol.* **29,** 1–17.
14. Soker, S., Fidder, H., Neufeld, G. & Klagsbrun, M. (1996) *J. Biol. Chem.* **271,** 5761–5767.
15. Gitay-Goren, H., Soker, S., Vlodavsky, I. & Neufeld, G. (1992) *J. Biol. Chem.* **267,** 6093–6098.
16. Gechtman, Z., Alonso, J. T., Raab, G., Ingber, D. & Klagsbrun, M. (1999) *J. Biol. Chem.* **274,** 28828–28835.
17. Bucana, C. D., Radinsky, R., Dong, Z., Sanchez, R., Brigati, D. J. & Fidler, I. J. (1993) *J. Histochem. Cytochem.* **41,** 499–506.
18. Radinsky, R., Bucana, C. D., Ellis, L. M., Sanchez, R., Cleary, K. R., Brigati, D. J. & Fidler, I. J. (1993) *Cancer Res.* **53,** 937–943.
19. Wilkinson, D. G. (1998) *In Situ Hybridization: A Practical Approach*, ed. Wilkinson, D. G. (Oxford Univ. Press, New York).
20. Dong, Z., Greene, G., Pettaway, C., Dinney, C. P. N., Eue, I., Lu, W., Bucana, C. D., Balbay, M. D., Bielenberg, D. & Fidler, I. J. (1999) *Cancer Res.* **59,** 872–879.
21. Giger, R. J., Urquhart, E. R., Gillespie, S. K. H., Levengood. D. V., Ginty, D. D. & Kolodkin, A. L. (1998) *Neuron* **21,** 1079–1092.
22. Kendall, R. L. & Thomas, K. A. (1993) *Proc. Natl. Acad. Sci. USA* **90,** 10705–10709.
23. Petch, L. A., Harris, J., Raymond, V. W., Blasband, A., Lee, D. C. & Earp, H. S. (1990) *Mol. Cell. Biol.* **10,** 2973–2982.
24. Lee, H. & Maihle, N. J. (1998) *Oncogene* **16,** 3243–3252.
25. Johnson, D. E., Lu, J., Chen, H., Werner, S. & Williams, L. T. (1991) *Mol. Cell. Biol.* **11,** 4627–4634.
26. Dvorak, H. F., Sioussat, T. M., Brown, L. F., Berse, B., Nagy, J. A., Sotrel, A., Manseau, E. J., Van de Water, L. & Senger, D. R. (1991) *J. Exp. Med.* **174,** 1275–1278.
27. Plate, K. H., Breier, G., Weich, H. A. & Risau, W. (1992) *Nature (London)* **359,** 845–848.
28. Kim, K. J., Li, B., Winer, J., Armanini, M., Gillett, N., Phillips, H. S. & Ferrara, N. (1993) *Nature (London)* **362,** 841–844.
29. Millauer, B., Longhi, M. P., Plate, K. H., Shawver, L. K., Risau, W., Ullrich, A. & Strawn, L. M. (1996) *Cancer Res.* **56,** 1615–1620.
30. Lin, P., Sankar, S., Shan, S., Dewhirst, M. W., Polverini, P. J., Quinn T. Q. & Peters, K. G. (1998) *Cell Growth Differ.* **9,** 49–58.
31. Goldman, C. K., Kendall, R. L., Cabrera, G., Soroceanu, L., Heike, Y., Gillespie, G. Y., Siegal, G. P., Mao, X., Bett, A. J., Huckle, W. R., *et al.* (1998) *Proc. Natl. Acad. Sci. USA* **95,** 8795–8800.
32. Kendall, R. L., Wang, G. & Thomas, K. A. (1996) *Biochem. Biophys. Res. Commun.* **226,** 324–328.
33. Benjamin, L. E. & Keshet, E. (1997) *Proc. Natl. Acad. Sci. USA* **94,** 8761–8766.